Suitability and characterization of pumice, bauxite, and ferrochrome slag as alternative raw materials in vitrified ceramic industry

Yunus Emre Benkli, **Kazım Koca**

Atatürk University, Faculty of Engineering, Department of Metallurgical and Materials Engineering, Erzurum, TÜRKİYE

Corresponding author: yebenkli@atauni.edu.tr (Yunus Emre Benkli)

Abstract: Since the natural raw materials used in the manufacture of clay-based ceramic products vary greatly in the sintering stage, the resulting products are quite heterogeneous. In addition, different types of waste could be used to make ceramic tiles and bricks. Therefore, this study aimed to investigate the effects of pumice, bauxite, and ferrochrome slag on the vitrified ceramic body. In this context, firstly, binary slip mixtures were prepared by composing 40% clay with 60% pumice, bauxite, and ferrochrome slag one by one, which was reduced to 150 µm in particle size. Then, the mixtures were shaped by slip casting method and sintered at 1000°C, 1100°C, 1200°C, and 1250°C. The qualitative XRD analysis was performed in order to see the phase variation, and physical properties were determined with shrinkage and water adsorption measurements. Since pumice transformed into a glassy phase after sintering at 1100°C, an amorphous phase was observed in all samples produced with pumice. In addition, the mullite development occurred in clay-pumice body composition with the temperature increment. However, tridymite and cristobalite phases were analysed in clay bauxite and ferrochrome body compositions. The shrinkage and water adsorption values, which were high in the samples sintered at 1000°C, began to reduce from 1100°C to 1250°C significantly. In particular, water adsorption reached 0% in the clay-pumice system which was suitable for a fully vitrified-high density standard (ISO13006-10545/98). Besides, the brighter colour was reached in the clay-pumice system while brown and black colour was seen in clay-bauxite and clay-ferrochrome bodies, respectively.

Keywords: vitrified ceramics, pumice, ferrochrome slag, bauxite, industrial waste

1. Introduction

Traditional ceramic production requires a large amount of natural raw materials since it is based mainly on the clay-silica-feldspar system. Natural raw materials used in the manufacture of clay-based ceramic products vary widely in terms of their composition, hence the resulting products are very heterogeneous. Such products can tolerate further compositional fluctuations and changes in raw materials, allowing different types of waste to be included in the internal structure of ceramic tiles and bricks as part of their matrix (Andreola et al., 2016).

Various studies on traditional ceramic making in recent years are related to the substitution of traditional raw materials with other natural resources such as zeolites (Gennaro et al., 2003; 2007), volcanic rocks (Carbonchi et al., 1999; Ergul et al., 2007), and nepheline syenite (Salem et al., 2009). With the increasing rate of industrialization, industrial waste is increasing significantly. Industrial waste, often accumulating outdoors, occupies a wide area and increases the cost of operation. All also cause severe environmental pollution and health hazards.

The use of various wastes in the manufacture of ceramic products has been proven to be beneficial both economically and environmentally (Durgut et al., 2015; Andreola et al., 2016). This typically includes industrial and agricultural wastes (Hoseny et al., 2018). The usage of industrial wastes particularly soda-lime glass fragments (Tucci et al., 2004), cathode ray tube, TV or a PC monitor (CRT Glass) (Andreola et al., 2008; 2010), granite cutting sludge (Torres et al., 2004), whiteware waste (Tarvornpanich et al., 2005), plumbing (Jackson et al., 2015), clay sewer pipes (El-Shimy et al., 2014),

construction waste (Jani and Hogland, 2014; Islam et al., 2017), and industrial residues from the polishing process (Rambaldi et al., 2007) has been investigated in the literature.

In agricultural wastes, the use of Si-rich wastes such as rice shell ash, which may be an alternative to quartz, was emphasized (Prasad et al., 2003). Besides, waste rocks, ore residues, and metallurgical wastes are industrial wastes that have the potential to cause serious economic, ecological, and health problems. These wastes can be considered alternative wastes in ceramic production, characterized by a high tendency to crystallize.

More recent studies have focused on alternative waste characterized by a high tendency to crystallize. In this way, the crystallinity of the final ceramics was increased. This effect can be achieved by using glass-ceramic frits (Zanelli et al., 2008) or wastes (Karamanova et al., 2011; Schabbach et al., 2012), which tend to crystallize highly. In this case, due to the processes of re-crystallization during the sintering and cooling stages, the amount of amorphous phase decreases and leads to improvement in mechanical properties (Zanelli et al., 2008).

In the production of vitrified ceramics (medical instrumentation), inorganic raw materials such as clay, feldspar, and quartz are mixed in certain ratios with the help of water to make sludge. After, synthetic resin or gypsum is poured into molds to be shaped. In the porcelain sintering process, mullite is the main crystal along with an amorphous phase in porcelain composition which the clay minerals are the basic source. The pure clay transformation begins with kaolinite-metakaolin transformation at 550°C and the metakaolin changes into spinel at 980°C, then the spinel turns into the kinds of mullite (Type I, Type II, Type III) crystals after 1000°C (Çevikel, 2010; Romero and Pérez, 2015; Gajek et al., 2017). In this process, there is residual amorphous silica which has nearly 1700°C of melting point (Wypych, 2016). However, the melting point of amorphous silica can be reduced to nearly 1100°C depending on the material and process parameters such as the ratio and type of fluxing agent, particle size distribution, specific pressure of shaping, etc (Darken, 1948; Niibori, 2000).

Research has been focusing on using pumice, and other industrial wastes as an alternative to raw materials that have been used in vitrified ceramics such as kaolin, feldspar, quartz, and albite. Increasing the availability of pumice and waste will lead to a decrease in the search for raw materials in the vitrified ceramics industry. Çelik and Yılmaz (2018) determined that the pumice did not change the amount of plasticity water of the clay, reducing the total shrinkage value, drying shrinkage, density, and fire loss. They determined that the reduction in the size of the pumice grains also reduced the water absorption ratio. As a result of this research, they found that the contribution of the pumice increased the strength of the final product with the decrease in grain size. They indicated that the contribution of alkaline pumice, decreased plasticity water, total shrinkage values, and frost resistance has changed insignificantly. The addition of pumice increased the water absorption ratio, and the coarser pumice grains showed that this ratio was higher (Deniz et al., 2004).

Ferrochrome slag does not contain free chromium oxide, and all components of ferrochrome slag are handily soluble in glass melts. Ferrochrome slag has a similar chemical composition to cordierite. Both mainly contain silicium (Si), manganese (Mg), and aluminum (Al). Slag also contains metallic elements such as iron (Fe), titanium (Ti), and heavy metals such as chromium (Cr), cobalt (Co), and nickel (Ni) (Liu et al., 2016). A study on the development of vitreous ceramic tiles related to ferrochrome slag, slag used in weight with other ceramic raw materials around 30-40%, sintered in the range of 1100-1150°C and sintered products showed relatively higher density with good strength properties. The properties of ferrochrome slag aggregate concrete explain that compared to broken limestone, reinforced aggregates of ferrochrome slag are better than limestone aggregates (Sahu et al., 2016).

The ceramic products need to be shaped and have green/dried strength till reaching the sintering process. Clayey raw materials are used 30-40% by weight to give such properties to the ceramic bodies in the industry and have no alternative to today's technology. Nowadays, the depletion of conventional raw materials and growing prices lead producers to research and use different kinds of local raw materials and industrial wastes in vitrified ceramic body compositions. As a consequence, new compositions are being researched to use such materials in ceramic body recipes but no adequate research studies can be found in the literature about the use of alternative raw materials and wastes in fully vitrified ceramic bodies. In this context, it was aimed to research the effects of pumice, bauxite,

and ferrochrome slag as alternatives for quartz and feldspathic materials in the production of fully vitrified ceramic bodies in terms of sintering properties.

2. Materials and methods

2.1. Materials

Pumice, bauxite, and ferrochrome slag samples were supplied by Erzurum-Kalebloksbims, Konya-Seydişehir Eti Aluminum, and Elazığ-Eti Chrome factories, Türkiye, respectively. The analysis results obtained from the pumice, bauxite, and ferrochrome slag samples dried at 105°C using the IQ+ non-standard program of the Philips brand Axions model XRF spectrometer are given in Table 1.

Table 1. Chemical analysis results of samples used in experimental studies

Content by wt. (%)	Pumice	Bauxite	Ferrochromium Slag (FeSiCr)
SiO_2	70.5	6.40	45.62
Al_2O_3	13.6	50.00	31.90
Fe_2O_3	1.9	16.25	1.95
TiO_2	0.2	2.55	0.03
CaO	0.8	0.46	2.25
MgO	0.3		16.80
MnO	0.1		0.01
K_2O	4.65		0.59
Na_2O	3.6		0.08
P_2O_5	0.1		0.01

2.2. Methods

A Union Process brand attritor device was used to grind the clay, pumice, and ferrochrome slag samples and to provide homogeneous mixtures of the ground raw materials. The samples were subjected to dry grinding for an average of 12 hours.

In the grinding stage, 1/8–1/4 inch ceramic balls were used, and the ball/raw material ratio was kept constant at 3/1 and the frequency at 60 Hz operating conditions. As a result of the grinding process, 80% of the products have passed below 150 µm. (d80 = 150 µm). Molds shown in Fig. 1 (a) were used for the slip casting of vitrified ceramic sludge. The molds used are made of gypsum due to their advantages, such as being porous and absorbing water equally on all sides. The casting process was carried out at a casting density of 1800 gr/lt. The products obtained at the end of the casting are shown in Fig. 1(b). The products obtained at the end of the casting were dried at 205°C for 1 hour. After the drying process, the samples were sintered for 8 hours in a PLF Series Protherm branded laboratory scale high-temperature furnace at temperatures of 1100°C, 1200°C, and 1250°C, respectively. After the sintering temperatures were reached, controlled cooling was started. The cooling process lasted an average of 24 hours, and the samples were taken out of the oven when the oven temperature was about 150–200°C.
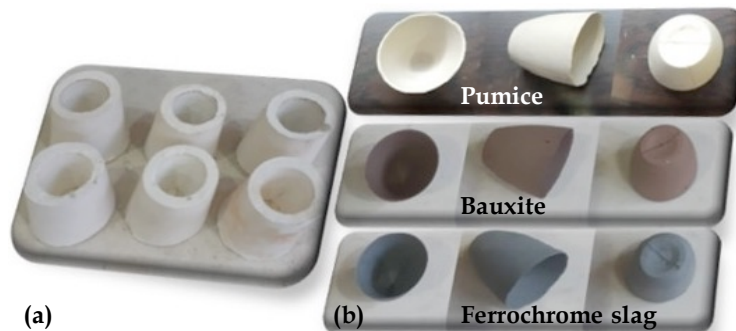

Fig. 1. (a) Gypsum mold for slip casting, (b) products obtained at the end of the casting

Water absorption and shrinkage analysis were executed according to TS EN ISO 10545 with 5 samples of 10x10 cm in size cut from sintered samples.

Konica Minolta CM-3600D spectrophotometer that had a 360 - 740 nm wavelength range and 10 nm wavelength interval was used for analyzing the color values of the specimens. The color values (L, a, b) were measured by scanning the surface, and three analyses were executed for each specimen with 0.08 average color measurement accuracy (ΔE).

XRD analyses were carried out using a Panalytical brand X-ray diffractometer device, using Cu Kα radiation (λ=1.54060 Ao) obtained by applying 45 kV voltage and 40 mA current to the Cu tube. We complete the measurements by scanning the sample surfaces at an angle of 2θ with a scanning speed of 20/min.

It used a Zeiss-brand Sigma 300 model scanning electron microscope at 15 kV to observe the morphology of the crystals and the number of crystals formed after the samples had been sintered. For the chemical analysis of the crystals formed in the sample, it used energy scattering X-ray spectrometry (EDX) operating in conjunction with the microscope. The samples were placed in a gold plating device before SEM.

3.   Results and discussion

3.1. Shrinkage ratios of sintered samples

In fully vitrified body composition systems containing clay minerals, approximately 1100°C is known as the temperature at which the initial phase of sintering begins and the first amorphous and mullite phases start to form (Romero and Pérez, 2015). At this point, the formation of the amorphous phase and the development of mullite phases are two mechanisms operating simultaneously. After this point, as the temperature increases, the reaction between the clay and the amorphous phase and the formation of mullite develop and the body begins to shrink with the sintering rate (Sallam and Chaklader, 1978). Table 2 and Figs. 2(a), (b), and (c) show the shrinkage rates in the length and width of the samples sintered at temperatures of 1000-1250 °C.

As seen from Figs. 2(a) and (b), as the sintering temperatures increase, the sintering shrinkage ratio in the height and width (base) of the samples increases. The width/height ratio of samples with a starting width/height ratio of 1/2 changes by 1/2 after sintering. As the alkali content in ceramic composition increases, the body hardens and shrinks up to a certain temperature according to material and process parameters (Carty and Senepati, 1998). After a certain temperature, deformation occurs which causes loss of quality in the product due to the decrease in the liquid phase viscosity of the body (Andreev and Zakharov, 2009). As seen in Figs. 2a and 2b, the body reaches maximum shrinkage at 1200°C with the increase in temperature due to the sodium and potassium contents in the body melting the quartz and, on the other hand, the development of mullite formation in the clay-pumice system (Weill and Kudo, 1968). Also, the clay-bauxite system showed a similar height-width shrinkage trend due to the iron content that acted as a fluxing agent for glass-forming oxide (Shute and Badger, 1942). For the clay-ferrochrome slag system, the height and width shrinkage showed important increments from 1200°C and 1100°C, respectively. In Fig. 3, it was seen that the fire shrinkage values were not affected so much for the three materials. It was also observed that the sintering shrinkage had the maximum value for all samples that occurred at 1250°C.

Ceramic clay shrinks when dried, and shrinks again when fired. Shrinkage during firing is due to the structure becoming non-porous and condensing. Water absorption percentage is related to porosity and how much water the sintered body can absorb. Most ceramic artists bake ceramic bodies at low temperatures to ensure a low shrinkage rate. However, porosity also increases to that extent. Shrinkage is highest when the stem is non-porous and dense.

The samples made with binary mixtures were also subjected to fire shrinkage experiments at different temperatures. After sintering at four different temperatures, the weights of binary mixtures were measured, and the fire shrinkage ratios were determined. It was observed from Fig. 2c that the fire shrinkage ratio increased at 1000°C, 1100°C, and 1200°C in 60% pumice and 40% clay mixture, while it decreased at 1250°C. That showed that the pumice was in the glassy phase after 1200°C. The gaps in the structure decreased to prevent fire shrinkage. The ratio of fire shrinkage decreased at the transition from 1000°C to 1100°C in a binary mixture of clay with bauxite and ferrochromium slag. This indicated that

the sintering temperature was insufficient at 1000ºC in the binary mixtures of bauxite and ferrochrome slag with clay. Ferrochrome slag had the lowest ratio of fire shrinkage as in the sintering shrinkage.

Table 2. The results of shrinkage ratios of sintered samples at temperatures of 1000-1250ºC

	Temperature (ºC)	Repetition	Pumice (%)	Average (%)	Bauxite (%)	Average (%)	Slag (%)	Average (%)
HEIGHT SHRINKAGE	1000	1	3.64	4.29	2.77	2.78	2.85	2.78
		2	4.94		2.79		2.71	
	1100	1	6.48	7.14	2.96	2.86	2.87	2.86
		2	7.80		2.76		2.85	
	1200	1	9.95	10.96	8.88	8.57	3.07	2.94
		2	11.97		8.26		2.81	
	1250	1	10.74	11.11	11.86	11.43	5.37	5.88
		2	11.48		11.00		6.39	
WIDTH SHRINKAGE	1000	1	1.09	1.33	0.00	0	0.82	0.67
		2	1.57		0.00		0.52	
	1100	1	3.00	2.67	1.35	1.33	0.83	0.68
		2	2.34		1.31		0.53	
	1200	1	5.67	5.33	5.97	6	2.62	2.67
		2	4.99		6.03		2.72	
	1250	1	6.27	6.67	6.24	6.68	3.45	3.33
		2	7.07		7.11		3.21	
FIRE SHRINKAGE	1000	1	5.67	5.43	11.33	11.17	4.19	4.15
		2	5.19		11.01		4.11	
	1100	1	6.11	6.22	10.26	10.13	3.35	3.40
		2	6.33		10.00		3.45	
	1200	1	7.07	6.57	11.56	11.29	4.20	4.30
		2	6.07		11.02		4.40	
	1250	1	5.10	5.79	12.84	12.85	5.09	4.84
		2	6.48		12.86		4.59	

3.2. Water absorption ratios of binary mixtures

The casting mud used in the production of ceramic sanitary ware is called Vitreous-China (Ural, 2007; Canduran and Ural, 2019). In its simplest definition, vitreous china is a sludge with a water absorption of less than 1%. Since fully vitrified body composition is used in ceramic sanitary ware that is in intense contact with water, such as toilets and bathrooms, water absorption value is of great importance and the standard water absorption value should be at most 0.5% (Fortuno, 2000) and it is determined with the fully vitrified body standard (ISO13006-10545/98). If the material absorbs water above this value, the water fills the pores in the product over time, causing cracks due to the thermal expansion and staining by fine-sized contaminants which reduces product functionality and quality. For this reason, the temperature at which 0.5% water absorption value is observed is called the firing temperature. Cups, bowls, and similar functional containers generally have high water absorption. Binary mixtures formed at different temperatures (1000ºC, 1100ºC, 1200ºC, and 1250ºC) were subjected to water absorption experiments. The results of the water absorption measurements are presented and shown in Table 3 and Fig. 3, respectively.

As seen in Fig. 3, the increased sintering temperatures lowered the water absorption ratio for each sample. the porous structure of the clay-pumice body showed contrast characteristics compared to the state after sintering and pumice had lower water adsorption from both bauxite and ferrochrome slag

which showed a less porous structure. The alkaline contents such as potassium and sodium in the pumice composition provided a lower melting point, therefore the water adsorption was decreased importantly with temperature increment (Tore, 2013; Durgut et al., 2022). Finally, the water absorption ratio was reduced to 0% because the pores in the vitrified ceramic sludge created by the pumice were entirely closed at 1250°C.
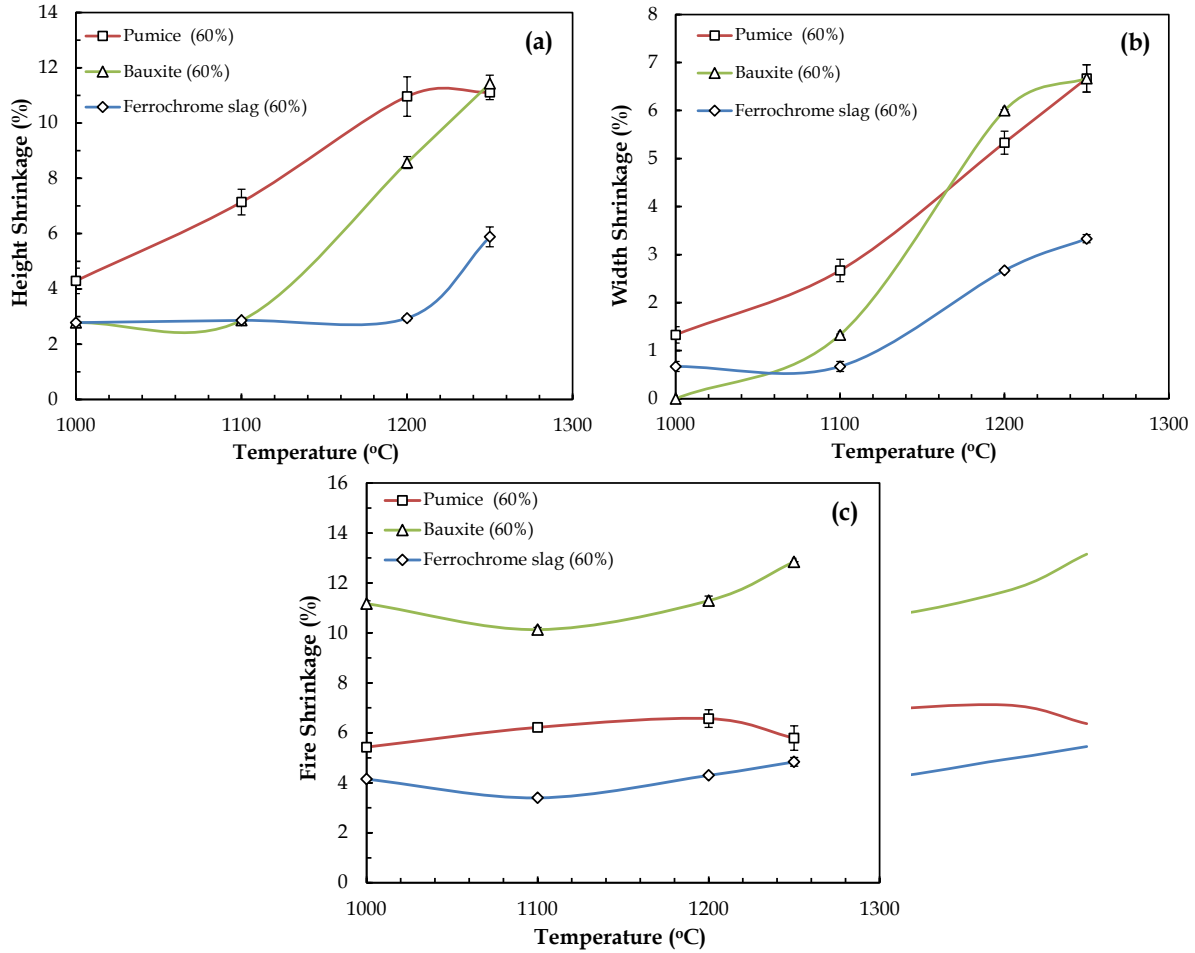

Fig. 2. Sintering and fire shrinkage values of the samples as a function of temperature (a) height, (b) width, and (c) fire

Table 3. The results of water absorption measurement at temperatures of 1000-1250°C

	Temperature (oC)	Repetition	Pumice (%)	Average (%)	Bauxite (%)	Average (%)	Slag (%)	Average (%)
WATER ABSORPTION	1000	1	16.89	16.93	23.07	23.04	21.16	21.25
		2	16.97		23.01		21.34	
	1100	1	2.38	2.27	18.02	18.02	23.75	23.92
		2	2.16		18.02		24.09	
	1200	1	0.50	0.6	13.99	13.85	18.12	18.18
		2	0.70		13.71		18.24	
	1250	1	0.00	0	12.12	12.07	17.98	17.86
		2	0.00		12.02		17.74	

3.3. XRD-SEM-EDX analysis of binary mixtures

XRD results for the P60K40 (60% Pumice, 40% San-B clay) sample as shown in Fig. 4. The appearance of the mullite phase strengthens the structure. Mullite is one of the most considerable phases in ceramics. The needle shape and the fact that the grains are very close to each other after sintering,

increase the strength values. It was seen that the quartz peaks were decreased and mullite peaks were increased with the temperature increment. This was due to the reaction with quartz (SiO_2) and Al-O content of pumice, so the peak variation showed the crystal formation change in the composition (Yuan et al., 2018).
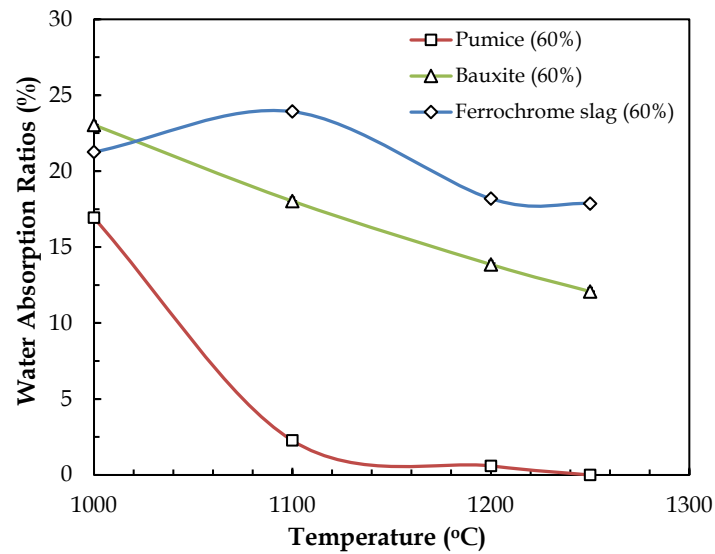

Fig. 3. Comparison of binary mixtures' water absorption ratios as a function of temperature
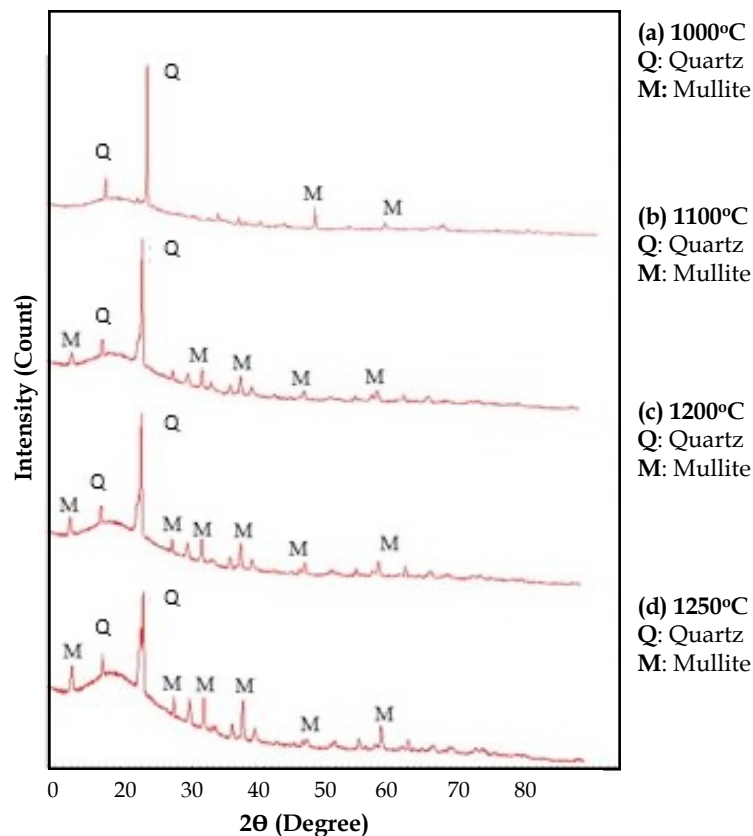

Fig. 4. XRD pattern of P60K40 sample sintered at different temperatures

EDS analyses and SEM images of the P60K40 (60% Pumice, 40% San-B clay) sample are given in Fig. 5 in which regional EDS data gathered from the P60K40 sample at 1000°C, 1100°C, 1200°C, and 1250°C sintering temperatures shows Al and Si elements predominantly. Elements such as Fe and Ti were in

very small quantities. Due to the high content of SiO_2 and Al_2O_3 in pumice and clay, excess quartz and mullite were observed at 1000°C, 1100°C, 1200°C, and, 1250°C in the XRD peak results given in Fig. 4.

In Fig. 5(a), the laminar shape, which looked like kaolinite minerals, was seen clearly in the composition. However, it was seen that the grains interacted more with each other and the body compactified with the increased temperature (1000°C, 1100°C, 1200°C, and 1250°C) in order of Fig. 5 (b), (c), (d). In Fig. 5c, the distribution of the Al_2O_3 and SiO_2 contents were seen in the SEM image given that were the indications of mullite and quartz formations at 1200°C sintering temperature, respectively.
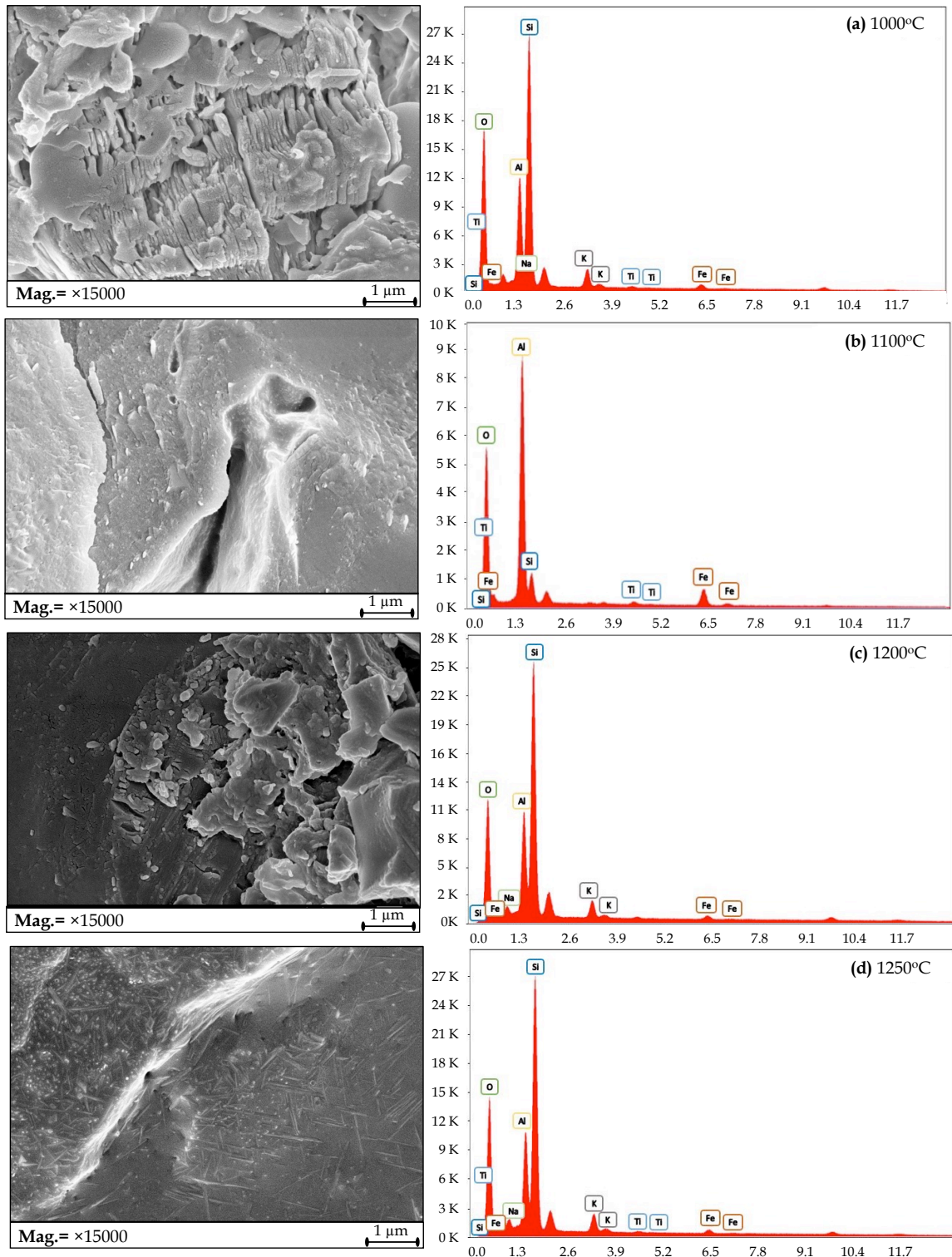

Fig. 5. SEM images and EDS analyses of P60K40 sample sintered at different temperatures (a) 1000°C, (b) 1100°C, (c) 1200°C, and (d) 1250°C

XRD results for the B60K40 (60% Bauxite, 40% San-B clay) sample are shown in Fig. 6. The existence of Al_2O_3 and SiO_2 oxides, as well as FeO and K_2O oxides in the B60K40 binary mixture, caused the formation of many phases (Fig. 6). The dominant phase quartz and the FeO phase also formed at 1000°C sintering temperature. The increased temperature (1100°C, 1200°C, and 1250°C) replaced quartz with different phases. The sintering temperature of 1000°C was not sufficient for the B60K40 sample. At 1100°C sintering temperature, it was seen that there were phases of mullite, rutile, potassium silicate, and cristobalite. At 1100°C sintering temperature, quartz was replaced with cristobalite. In the samples with pumice, an amorphous phase was observed, but no amorphous phase was found in the formation of bauxite with clay. Cristobalite is a silica mineral polymorph that occurs between metakaolin and mullite at 1050°C and can cause quality problems such as cracks in the cooling step of ceramic bodies due to the high thermal expansion coefficient property (Sato et al., 2000). Cristobalite becomes steady after the 1470°C temperature. However, when sintering at 1200°C, cristobalite crystallization occurs before quartz becomes tridymite. The cristobalite phase increases the coefficient of thermal expansion. Tridymite phase, which is the second polymorph of the silica formed at 1250°C sintering temperature (Hillig, 1993).

Tridymite is not used much in the industry. In general, it resembles cristobalite and is a low-density version of silica (Ateşer, 2010). The rutile phase usually affects color change in ceramics. Bauxite was observed to add a brownish color to samples. Mullite is the most dominant phase at 1250°C sintering temperature.
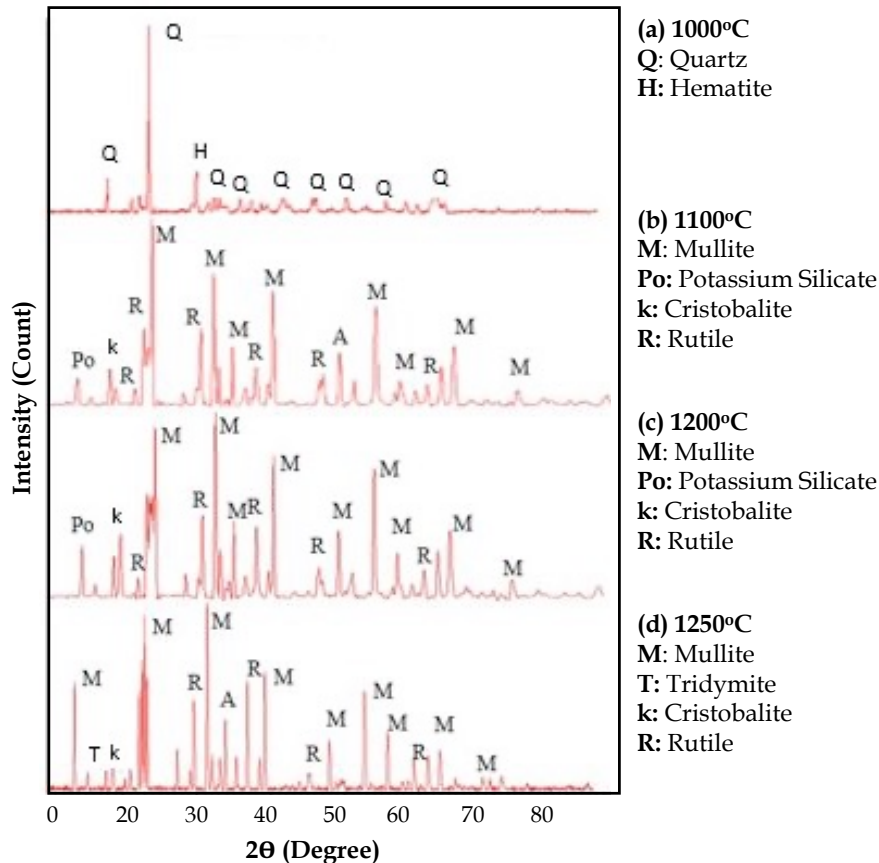

Fig. 6. XRD pattern of B60K40 sample sintered at different temperatures

EDS analyses and SEM images of the B60K40 (60% Bauxite, 40% San-B clay) sample at sintering temperatures of 1000°C,1100°C, 1200°C, and 1250°C are shown in Fig. 7. In the B60K40 binary mixture, the elements Al and Si were in high quantities. At the same time, Fe was determined at all sintering temperatures. Quartz, a polymorph of silica, forms into cristobalite and tridymite as temperature increases (1000°C, 1100°C 1200°C, 1250°C). The SEM image given in Fig. 7a shows rutile at 1000°C sintering temperature. The distribution of Al_2O_3 phases is observed at 1200°C sintering temperature (Fig. 7c) and mullite and SiO_2 phases are observed at 1250°C sintering temperature (Fig. 7d).
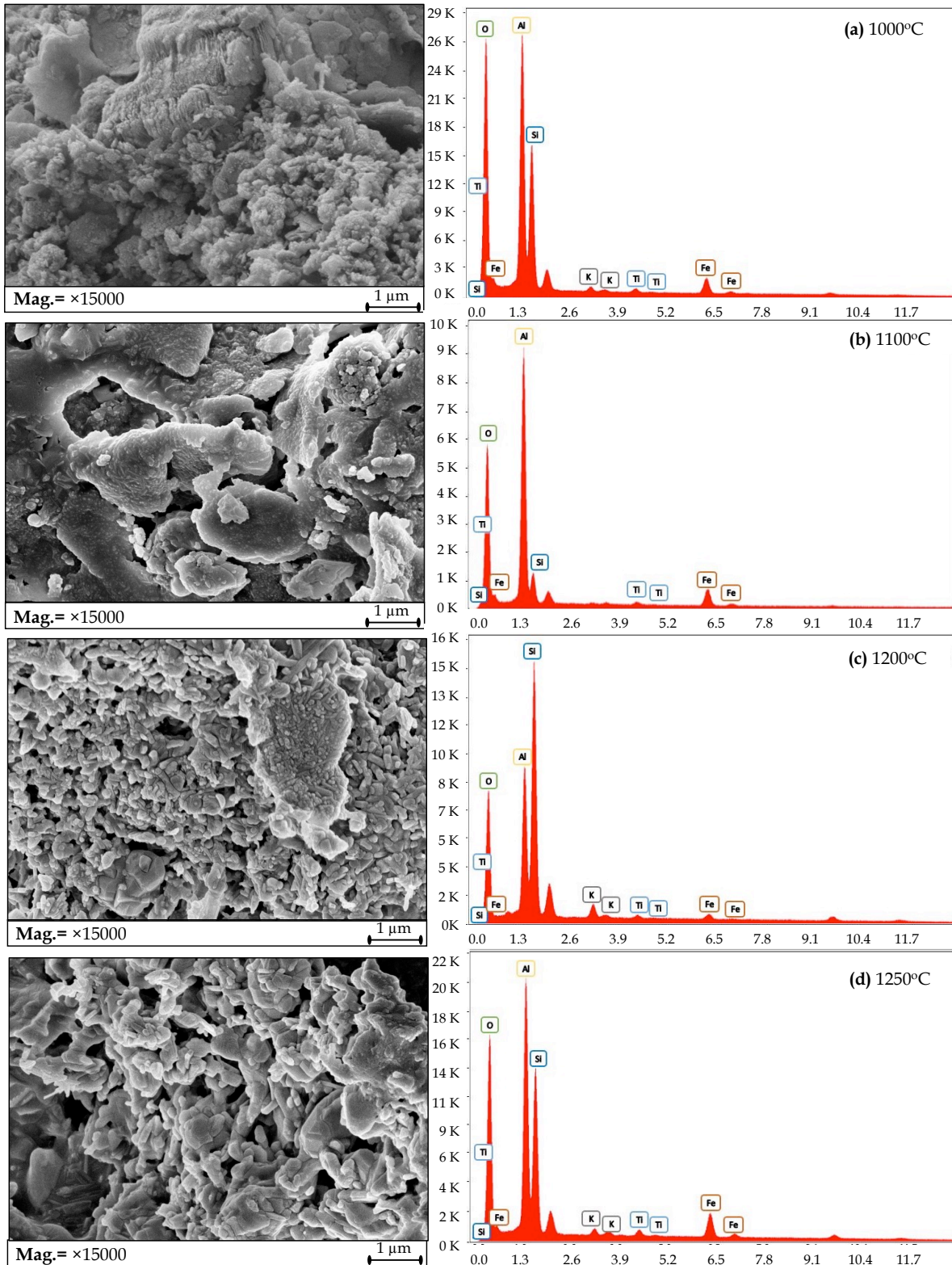
Fig. 7. SEM images and EDS analyses of B60K40 sample sintered at different temperatures (a) 1000ᵒC, (b) 1100ᵒC, (c) 1200ᵒC, and (d) 1250ᵒC

XRD results for the C60K40 (60% Ferrochrome slag, 40% San-B clay) sample are shown in Fig. 8. Al, SiO_2, and MgO crystals were predominant in the binary mixture C60K40 (Slag 60%, Clay 40%). SiO_2 (quartz) phase was observed at 1000ᵒC sintering temperature. 1000ᵒC sintering temperature was not sufficient for the C60K40 sample. SiO_2 and Al_2O phase, where the MgO phase is more predominant at

1200°C and 1250°C sintering temperatures respectively, is observed to be less than the MgO phase. At 1250°C and 2θ=28°, the most dominant peak was cordierite. The thermal expansion coefficients of cordierite were low. This feature gives ceramics mechanical and thermal shock resistance (Kiattisaksophon and Thiansem, 2008). It also provides ceramics excellent shock resistance, high thermal and chemical stability, low dielectric constant in the high-frequency zone, and large surface area in bulk porous structures (Davila et al. 2008; Kobayashi et al. 2000). Quartz phase was determined after 1200°C sintering temperature.

(a) 1000°C
F: Forsterite
m: Magnesium Aluminum Oxide

(b) 1100°C
F: Forsterite
m: Magnesium Aluminum Oxide
P: Potassium Aluminum Oxide

(c) 1200°C
m: Magnesium Aluminum Oxide
k: Cristobalite
Q: Quartz
C: Cordierite

(d) 1250°C
m: Magnesium Aluminum Oxide
k: Cristobalite
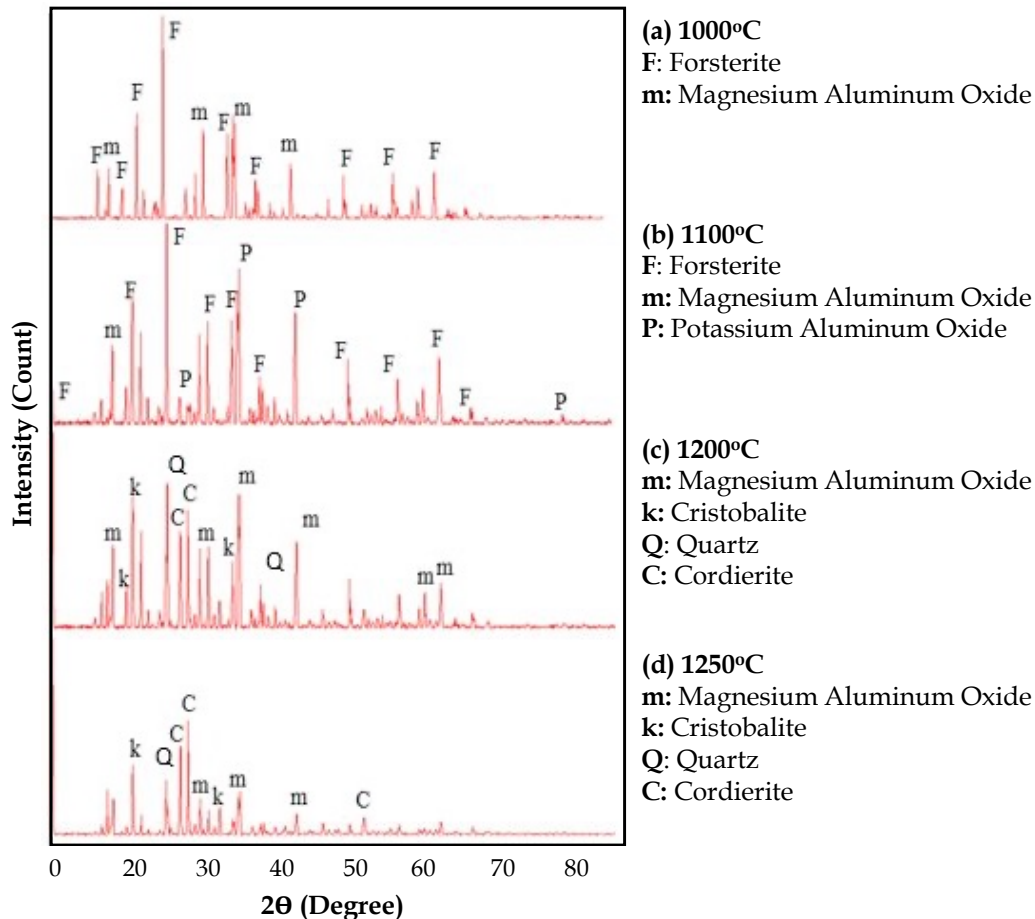**Q**: Quartz
C: Cordierite

Fig. 8. XRD pattern of C60K40 sample sintered at different temperatures

EDS analyses and SEM images of the C60K40 (60% Ferrochrome slag, 40% San-B clay) sample at different sintering temperatures are given in Fig. 9. Ferrochrome slag contains Mg and K besides Al and Si. Even if the composition was the same, the Fe content was determined in Fig. 9 (d) EDS analysis. In the XRD data given in Fig. 8 of the C60K40 sample, the cristobalite phase, which is the polymorph of quartz, and the quartz phase were observed at 1200°C and 1250°C. The cordierite phase was at the same temperatures. In the SEM images given in Figs. 9c and Fig. 9d (at sintering temperatures of 1200°C and 1250°C respectively), cordierite phases, and distribution of SiO phases at 1000°C, 1100°C, and 1250°C were also observed.

3.4. Colour measurements

Color measurements were made to determine the color values of the sintered products obtained as a result of the experiments. The data obtained as a result of the measurements are shown in Table 2 and Fig. 10.

In the Slag-Clay system, the phosphorite phase seen at 1000°C and 1100°C added a brown tone to the ceramic body. The forsterite phase is seen in the XRD analysis in Figs. 8a and 8b generally provide a color change in ceramics in brown tones (Arcasoy, 1983). The potassium content seen in the EDS analyses shown in Fig. 9 caused the color of the resulting product to be in gray tones. (Fig. 10b).
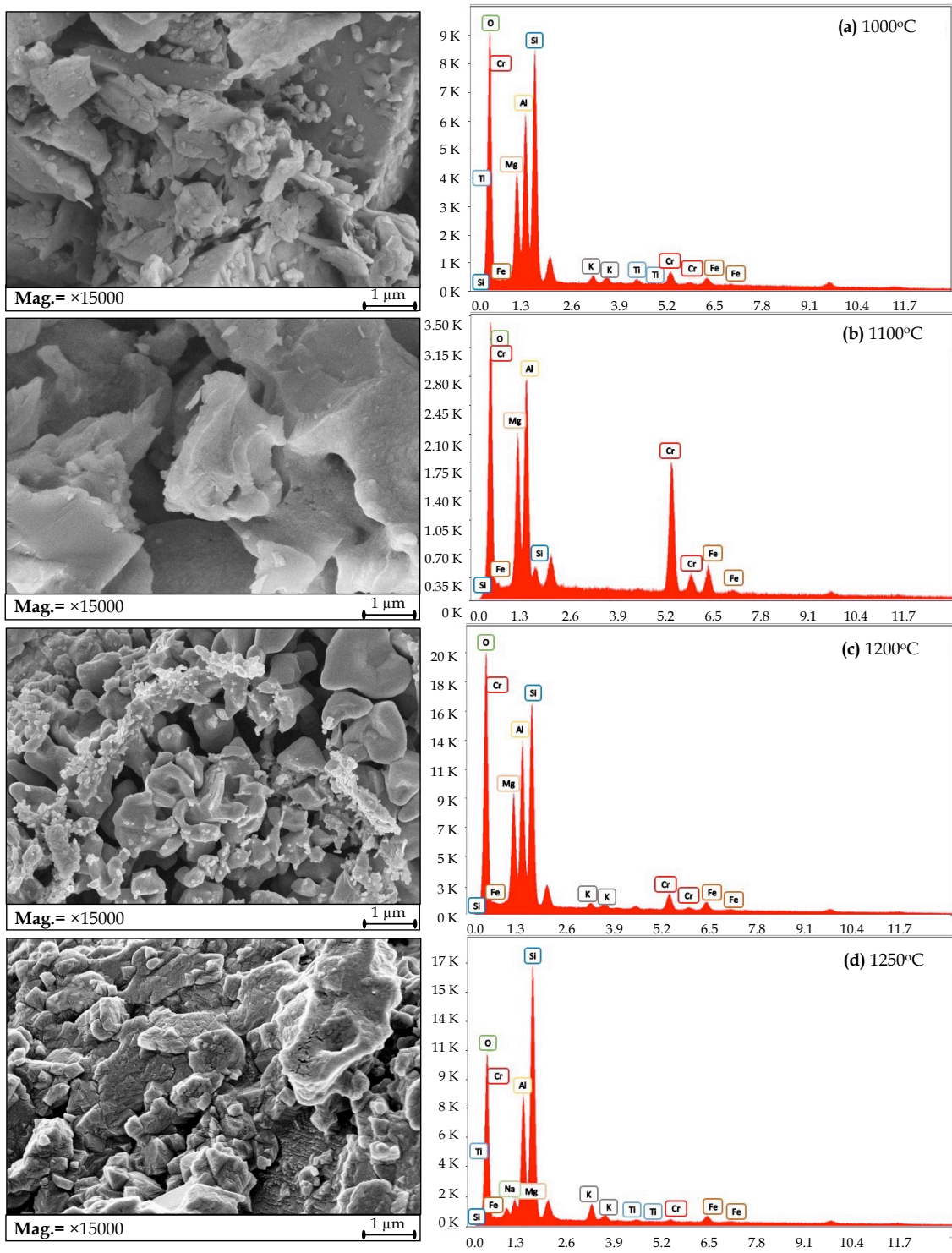
Fig. 9. SEM images and EDS analyses of C60K40 sample sintered at different temperatures (a) 1000°C, (b) 1100°C, (c) 1200°C, and (d) 1250°C

Table 4. L*a*b* values of the products obtained as a result of the experiments

	Pumice			Slag			Bauxite		
Temperature/Color	L	a	b	L	a	b	L	a	b
1000 °C	75.68	6.71	20.67	71.66	2.84	10.26	66.25	13.86	17.80
1100 °C	61.74	5.07	27.39	70.40	2.29	16.23	63.17	9.16	18.70
1250 °C	56.93	5.65	23.31	57.00	7.43	31.01	58.62	8.93	2.37

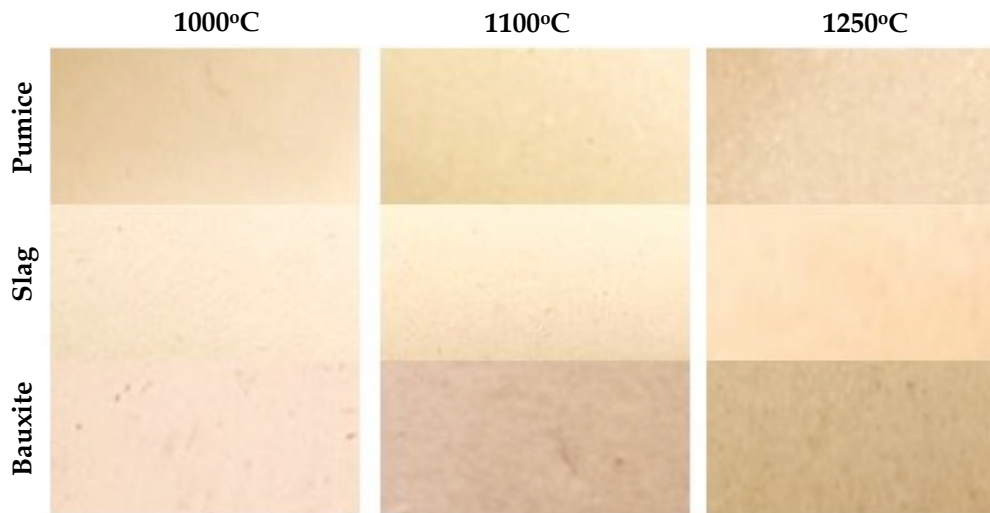|	1000°C	1100°C	1250°C
Pumice			
Slag			
Bauxite			

Fig. 10. Color scale of the products obtained as a result of the experiments

The cordierite phase, which appeared at 1250 °C in the XRD analysis in Fig. 8d, caused the yellow (b*) and red (a*) tones in the ceramic body to increase and the white balance (L*) to decrease. The cordierite phase darkens the firing color of ceramics in the presence of FeO in the structure. (Arcasoy A, 1983) With the emergence of the cordierite phase, the balance of yellow and red in the ceramic body, which had a brown tone, increased and the color of the ceramic structure changed from brown to yellow. (Fig. 10b)

While the light red tone was dominant in the color of the product obtained at 1000°C in the bauxite clay system, a color tone between yellow and cream was observed in the body as the sintering temperature increased. As seen in the rutile phase generally provides a yellow color change in ceramics due to its titanium content. (Arcasoy, 1983) As the sintering temperature increased, the color of the ceramic body began to darken.

4. Conclusions

Natural raw materials, which have become the biggest problem in the world, are decreasing every year. The decrease in the raw materials used in ceramics every year has led the industry and scientists to search for new raw materials. Many studies are being conducted on the use of pumice and other industrial wastes as alternatives to raw materials such as kaolin, feldspar, quartz, and albite used in vitrified ceramics. Additionally, continuous industrial activities produce increasing amounts of waste and by-products that are subject to environmental legislation. Recycling these wastes is of great importance, both to contribute to the country's economy and to prevent the depletion of natural resources. Some wastes are similar in composition to natural raw materials used in ceramic production. For this reason, although upgrading industrial wastes to alternative raw materials is technically and economically interesting, recycling wastes will also provide great advantages in terms of the economies of the countries and the reduction of environmental damage. The availability of pumice, bauxite, and waste will reduce the search for raw materials in the vitrified ceramic industry.

In this study, 40% clay, acidic pumice supplied from the Erzurum-Kalebloksbims factory, bauxite supplied from the Konya-Seydişehir Eti Aluminum factory, and ferrochrome slag supplied from Elazığ-Eti Chrome factory were prepared as binary mixtures separately. Prepared mixtures were poured into molds by slip casting method and sintered at 1000°C, 1100°C, 1200°C, and 1250°C, and vitrified ceramic samples were obtained. Then, these vitrified ceramic samples have been characterized.

It was seen that the shrinkage was increased with the temperature increment that showed vitrified body compaction because of the solid/liquid phase formation development. The most change was reached in the clay-pumice binary system due to the alkaline (Na_2O+K_2O) content which was the reason for lowering the eutectic point. Secondly, there was proximate shrinkage values were gained with the clay-bauxite binary system, the Fe_2O_3 content acted as a fluxing agent in the shrinkage value and also

the color change. Lastly, the lowest vitrification rate was observed in ceramics created with ferrochrome. The same phenomenon also occurred for water adsorption results. The glassy and crystal phase could not form enough at 1000°C and the water adsorption values were high for clay-pumice/bauxite/ferrochrome binary systems. However, after 1100°C clay minerals, free quartz, and alkaline content began to turn into glassy phase and mullite so the open porosity and the water adsorption reduced to 0% for clay/pumice composition. For the clay-bauxite and ferrochrome systems, it was observed that the water adsorption did not lower so much due to the lack of fluxing material in the composition. With the temperature increment, the quartz peak decreased and the mullite peak increased for the clay-pumice composition. However, quartz transformed into cristobalite and tridymite, also mullite and rutile development was detected for clay-bauxite composition. On the other hand, clay-ferrochrome composition resulted in magnesium aluminum oxide, cristobalite, quartz, and cordierite as formed phases.

In conclusion, the clay-pumice system showed vitrified ceramic body properties and gave brighter colour values to the final product. However, the cristobalite and tridymite contents, which occurred for sintered clay-bauxite and ferrochrome bodies, could cause thermal shock cracks because of the high thermal expansion coefficient, especially in glazed products. Again, the darker colour properties of clay-bauxite and clay-ferrochrome systems were the results of metal elements such as Fe, Ti, and Cr in the composition and were used to make dark-colored products.

Acknowledgements

References

ANDREEV, D.V., ZAKHAROV, A.I., 2009. *Deformation of porcelain articles*. Glass and Ceramics, 66(1), 8-10.

ANDREOLA, F., BARBIERI, L., KARAMANOVA, E., LANCELLOTTI, I., PELINO, M., 2008. *Recycling of CRT panel glass as fluxing agent in the porcelain stoneware tile production*. Ceramics International, 34(5), 1289-1295.

ANDREOLA, F., BARBIERI, L., BONDIOLI, F., FERRARI, A.M., LANCELLOTTI, I., MISELLI, P., 2010. *Recycling screen glass into new traditional ceramic materials*. International Journal of Applied Ceramic Technology, 7(6), 909-917.

ANDREOLA, F., BARBIERI, L., LANCELLOTTI, I., LEONELLI, C., MANFREDINI, T., 2016. *Recycling of industrial wastes in ceramic manufacturing, state of art and glass case studies*. Ceramics International, 42(12), 13333-13338.

ARCASOY, A., 1983. *Ceramic Technology*, Marmara University, Faculty of Fine Arts Publications, No, 2, Istanbul, 19, p, 228

ATEŞER, H.O., 2010. *Investigation of sintering and mechanical properties of amorphous silica ceramics with andalusite addition*. Thesis (M.Sc.), Istanbul Technical University, Institute of Science and Technology.

CANDURAN, K., URAL, M., 2019. *Apparatus used to prevent deformation in the production of ceramic sanitary ware*. Academic Art, 4(8), 66-79.

CARBONCHI, G., DONDI, M., MORANDI, N., TATEO, F., 1999. *Possible use of altered volcanic ash in ceramic tile production*. Industrial Ceramics, 19(2), 67-75.

CARTY, W.M., SENEPATI, U., 1998. *Porcelain-raw materials, processing, phase evolution, and mechanical behaviour*. Journal of the American Ceramic Society, 81, 3-20.

ÇELIK, M.Y., YILMAZ, S., 2018. *The effect of static, salty and acidic aqueous environments on the capillary water absorption potential of porous building stones used as building stones in the Afyonkarahisar region*. Journal of the Faculty of Engineering and Architecture of Gazi University, 33(2), 591-607.

ÇEVIKEL, Ü.İ., 2010. *Comparison of PVC, glass mosaic and ceramic tiles in terms of application as coating materials in private reinforced concrete swimming pools*. Thesis (M.Sc.), Istanbul Technical University, Institute of Science and Technology.

DARKEN, L.S., 1948. *Melting points of iron oxides on silica; phase equilibria in the system Fe-Si-O as a function of gas composition and temperature*. Journal of the American Chemical Society. 70(6), 2046-2053.

DAVILA, L.P., RISBUT, S.H., SHACKELFORD, J.F., 2008. *Quartz and Silicas*. Ceramic and Glass Materials, 71–86., Editors, Shackelford, J.F., Doremus, R.H.

DENIZ, V., UMUCU, Y., YILMAZ, I., 2004. *Evaluation of jig performances in the pumice enrichment facility of Soylu Industrial Minerals Inc.* 5 Endüstriyel Hammaddeler Sempozyumu, 307-312.

DURGUT, E., PALA, C.Y., KAYACI, K., ALTINTAS, A., YILDIRIM, Y., ERGIN, H., 2015. *Development of a semi-wet process for ceramic wall tile granule production*. J. Ceram. Process. Res., 16(5), 596–600.

DURGUT, E., CINAR, M., OZDEMIR, O., 2022. *Effect of calcite and mica contents in nepheline syenite samples on the ceramic body sintering behaviours and surface roughness*. Physicochemical Problems of Mineral Processing, 58(5), 149179.

EL-SHIMY, Y.N., AMIN, K., EL-SHERBINY, S.A., ABADIR, M.F., 2014. *The use of cullet in the manufacture of vitrified clay pipes*. Construction and Building Materials, 73, 452-457.

ERGUL, S., AKYILDIZ, M., KARAMANOV, A., 2007. *Ceramic material from basaltic tuffs*. Industrial Ceramics, 27(2), 211-217.

FORTUNO, D., 2000. *Firing*. Ceramic Technology Sanitaryware, Gruppo Editorialle Feanza Editrice S.P.A, Feanza, Italy, 125–126.

GAJEK, M., PARTYKA, J., KMITA, A.R., GASEK, K., 2017. *Development of anorthite based white porcelain glaze without zrsio4 content*. Ceramics International, 43(2), 1703-1709.

GENNARO, R., CAPPELLETTI, P., CERRI, G., GENNARO, M., DONDI, M., GUARINI, G., LANGELLA, A., NAIMO, D., 2003. *Influence of zeolites on the sintering and technological properties of porcelain stoneware tiles*. Journal of the European Ceramic Society, 23(13), 2237-2245.

GENNARO, R., DONDI, M., CAPPELLETTIC, P., CERRID, G., GENNARO, M., GUARINI, G., LANGELLA, A., PARLATOC, L., ZANELLI, C., 2007. *Zeolite-feldspar epiclastic rocks as flux in ceramic tile manufacturing mesoporous microporous mater*. Microporous and Mesoporous Materials, 105(3), 273-278.

HILLIG, W.B., 1993. *A methodology for estimating the mechanical properties of oxides at high temperatures.* Journal of the American Ceramic Society 76(1), 129-138.

HOSENY, N.F., AMIN, S.K., FOUAD, M.M.K., ABADIR, M.F., 2018. *Reuse of ceramic sludge in the production of vitrified clay pipes*. Ceramics International, 44(11), 12420-12425.

ISLAM, G.M.S., RAHMAN, M.H., KAZI, N., 2017. *Waste glass powder as partial replacement of cement for sustainable concrete practice*. Journal of Environmental Chemical Engineering, (3), 1767-1775.

JACKSON, P.R., HANCOCK, P., CARTLIDGE, D., MUKESH, C., LIMBACHIYA, J., ROBERTS, J., 2015. *Recycled bottle glass as a component of ceramic sanitary ware*. Sustainable Waste Management And Recycling, Glass Waste, ICE Publishing, 313-320.

JANI, Y., HOGLAND, W., 2014. *Waste glass in the production of cement and concrete – A review*. Journal of Environmental Chemical Engineering, 2(3), 1767-1775.

KARAMANOVA, E., AVDEEV, G., KARAMANOV, A., 2011. *Ceramics from blast furnace slag. kaolin and quartz*. Journal of the European Ceramic Society, 31(6), 989-998.

KIATTISAKSOPHON, P., THIANSEM, S., 2008. *The preparation of cordierite-mullite composite for thermal shock resistance material*. Chiang Mai J. Sci. 2008; 35(1), 6-10.

KOBAYASHI, Y., SUMI, K., KATO, E., 2000. *Preparation of dense cordierite ceramics from magnesium compounds and kaolinite without additives.* Ceramics International, 26(7), 739-743.

LIU, C., LIU, L., TAN, K., ZHANG, L., TANG, K., SHI, X. 2016. *Fabrication and characterization of porous cordierite ceramics prepared from ferrochromium slag*. Ceramics International, 42(1), 734-742.

NIIBORI, Y., KUNITA, M., TOCHIYAMA, O., CHIDA, T., 2000. *Dissolution rates of amorphous silica in highly alkaline solution*, Journal of Nuclear Science and Technology, 37(4), 349-357.

PRASAD, C.S., MAITI, K.N., VENUGOPAL, R. 2003. *Effect of the substitution of quartz by rha and silica fume on the properties of whiteware compositions*. Ceramics International, 29(8), 907-914.

RAMBALDI, E., ESPOSITO, L., TUCCI, A., TIMELLINI, G., 2007. *Recycling of polishing porcelain stoneware residues in ceramic tiles*. Journal of the European Ceramic Society, 27(12), 3509-3515.

ROMERO, M., PÉREZ, J.M., 2015. *Relation between the microstructure and technological properties of porcelain stoneware. A review*. Mater. Construcc. 65 [320], e065.

SAHU, N., BISWAS, A., KAPURE, G.U., 2016. *A short review on utilization of ferrochromium slag*. Mineral Processing and Extractive Metallurgy Review 37(4), 211-219.

SALEM, A., JAZAYERI, S.H., RASTELLI, E., TIMELLINI, G., 2009. *Dilatometric study of shrinkage during sintering process for porcelain stoneware body in presence of nepheline syenite*. Journal of Materials Processing Technology, 209(3), 1240-1246.

SALLAM, E.M.H., CHAKLADER, A.C.D., 1978. *Sintering characteristics of porcelain*. Ceramurgia International, 4 (4), 151-161.

SATO, T., SAWABE, Y., OHYA, Y., SUGAI, M., NAKAGAWA, Z., 2000. *Cracking in a cristobalite-containing mullite body during cooling*. Journal of the Ceramic Society of Japan 108(4), 345-349.

SCHABBACH, L.M., ANDREOLA, F., BARBIERI, L., LANCELLOTTI, I, KARAMANOVA, E., RANGUELOV, B., KARAMANOV, A., 2012. *Post-treated bottom incinerator bottom ash as alternative raw material for ceramic manufacturing*. Journal of the European Ceramic Society, 32(11), 2843-2852.

SHUTE, R.L., BADGER, A.E., 1942. *Effect of iron oxide on melting of glass.* Journal of the American Ceramic Society. 25(12), 355-357.

TARVORNPANICH, T., SOUZA, G.P., LEE, W.E., 2005. *Micro-structural evolution on firing soda-lime-silica glass fluxed white-wares*. Journal of the American Ceramic Society, 88(5), 1302-1308.

TORE, I., 2013. *Uses of pumice as alternative flux for floor tile products*. International Journal of Science and Modern Engineering. 1(11), 16, 19.

TORRES, P., FERNANDES, H.R., AGATHOPOULOS, S., TULYAGANOV, D.U., FERREIRA, J,M., 2004. *Incorporation of granite cutting sludge in industrial porcelain tile formulations*. Journal of the European Ceramic Society, 24(10–11), 3177-3185.

TUCCI, A., ESPOSITO, L., RASTELLI, E., PALMONARI, C., RAMBALDI, E., 2004. *Use of soda-lime scrap-glass as a fluxing agent in a porcelain stoneware tile mix*. Journal of the European Ceramic Society, 24(1), 83-92.

URAL, M., 2017. *Deformations occurring in vitrified ware production and their elimination*. Sakarya University, Institute of Social Sciences, Department of Ceramics and Glass (Master's Thesis), 141 pages, Sakarya, Türkiye.

WEILL, D.F., KUDO, A.H., 1968. *Initial melting in alkali feldspar-plagioclase-quartz systems*. Geological Magazine. 105(4), 325-337.

WYPYCH, G., 2016. *2 - Fillers – Origin, Chemical Composition, Properties, and Morphology*. Editor(s), George Wypych, Handbook of Fillers (Fourth Edition), ChemTec Publishing, Pages 13-266, ISBN 9781895198911.

YUAN, S., HAN, Y., LI, Y., GAO, P., YU, J., 2018. *Effect of calcination temperature on activation behaviors of coal-series kaolin by fluidized bed calcination*. Physicochemical Problems of Mineral Processing, 54(2), 590-600.

ZANELLI, C., BALDI, G., DONDI, M., ERCOLANI, G., GUARINI, G., RAIMONDO, M., 2008. *Glass ceramic frits for porcelain stoneware bodies, effects on sintering, phase composition and technological properties*. Ceramics International, 34(3), 455-465.